

Automated Optimization of Irregular Elliptical PinFin Heatsinks for SiC Power Module

Xiaoshuang Hui^[1,2] , Puqi Ning^[1,2] , Dongrun Li^[1,2], Yuhui Kang^[1], Fan Tao^[1,2] 

¹Key Laboratory of High Density Electromagnetic Power and Systems (Chinese Academy of Sciences), Institute of Electrical Engineering, Chinese Academy of Sciences, Haidian District, Beijing 100190, China;

²University of Chinese Academy of Sciences, Shijingshan District, Beijing 100049, China

Corresponding author: Puqi Ning, npq@mail.iee.ac.cn

Speaker: Xiaoshuang Hui, hui00@mail.iee.ac.cn

Abstract

Enhancing the heat dissipation performance of SiC power modules plays a crucial role in the overall performance of motor drives. In this paper, an automatic optimization design method for PinFin heat sink with irregular layout is proposed for SiC power modules. Firstly, a coding method is introduced to automatically generate candidate layouts of elliptical PinFin with random arrangements of rotation direction, size, and spacing. Secondly, the lattice Boltzmann method (LBM) is employed to evaluate the elliptical PinFin performance. Finally, genetic algorithm (GA) is utilized to select optimal layouts from candidate encodings, and the optimized heat sink is fabricated and welded onto the three-phase SiC power module. Simulation and experimental results demonstrate that the junction temperature of the power module with optimized Irregular Elliptical PinFin is reduced by more than 4 °C under a three-phase series-connected continuous current of 180A, validating the effectiveness of the proposed optimization method in this paper.

1 Introduction

The development of the new energy vehicle (NEV) industry has raised higher demands for the drive systems of electric vehicles. Silicon Carbide (SiC) devices, with their low losses, high-temperature tolerance, and high-frequency operation capabilities, are advantageous technologies that facilitate the doubling of power density in electric drive systems^[1,2]. Thermal management plays a critical role in the performance of motor drives, as heat generated from power module losses is a primary concern. Therefore, optimizing power module heatsinks is crucial to enhancing the overall performance of the motor drive system^[3,4].

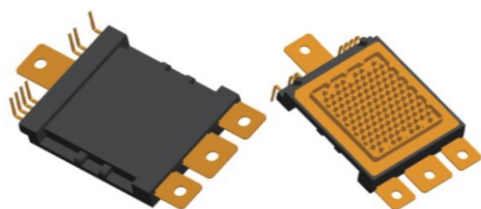


Fig. 1. SiC power module with PinFin heatsink

In recent years, mainstream SiC power module products commonly use PinFin heat sinks, as shown in Fig. 1^[5]. These heat sinks feature numerous cylindrical or pin-like protrusions designed to maximize the contact surface area between the heat sink and the cooling medium flowing over its surface. This configuration significantly improves heat exchange efficiency^[6].

Therefore, there is still significant untapped potential in PinFin heat dissipation performance, which can effectively enhance SiC device performance further. Ref [7] designed a PinFin variable density topology optimization model, aiming for multi-objective optimization with thermal resistance and coolant pressure drop as targets. Ref [8] found that elliptical PinFin exhibit superior heat dissipation performance due to their larger convective surface area. Ref [9] developed an optimization method for PinFin with unequal heights and spacing. Ref [10] proposed an automatic optimization method and process for heat sinks.

This paper presents a coding method to automatically generate effective layouts of elliptical PinFin with different rotation angles, sizes, and random positions. Subsequently, the Lattice Boltzmann Method - Large

This work was supported in part by National Key R&D Program of China (2021YFB2500600), and in part by CAS Youth multi-discipline project (JCTD-2021-09).

Eddy Simulation (LBM-LES) is utilized to calculate the flow velocity and pressure of elliptical PinFin. These calculations are combined with a pump to find the working point velocity as an optimization fitness. Genetic algorithms are employed for selection, and the optimized irregular elliptical PinFin heat sink is manufactured and welded onto a three-phase half-bridge SiC power module for experimental validation.

2 Proposed Automated Optimization Methodology

2.1 Encoding Initialization

To automatically generate candidate solutions for irregular PinFins with different rotation angles, sizes, and random positions, an encoding method is proposed. As illustrated in the Fig. 2, the encoding of irregular PinFins consists of five parts: sequence weight, displacement distance in the x-direction and y-direction, ellipse size, and rotation angle. The ellipses are sequentially displaced in the x-direction and y-direction, followed by changes in size and rotation angle. For simplicity, there are several options available for rotation angles to choose from, rather than all angles. In case of conflicts in ellipse positions, the one with higher sequence weight is retained.

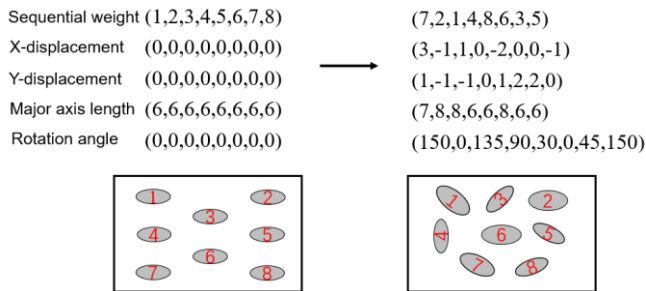


Fig. 2. Encoding of Irregular PinFins

During the crossover process, the encoding uses the longest common subsequence (LCS) crossover method. First, the longest common subsequence in the sequence weight chromosomes (parents) is identified and its positions are kept fixed. Next, the numbers outside the longest sequence are exchanged sequentially, as shown in Fig. 3. The remaining encoding elements are exchanged based on the exchange points of the sequence weights.

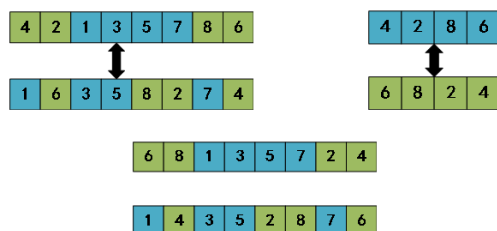


Fig. 3. Procedure of LCS crossover method

Before optimization, the initial population of individuals is randomly generated. During the genetic operations, if the number of ellipses in the offspring is less than the specified limit, new ellipses will be randomly added to. Genetic operations ensure that the offspring maintains effective layout characteristics inherited from the parent, as illustrated in the Fig. 4.

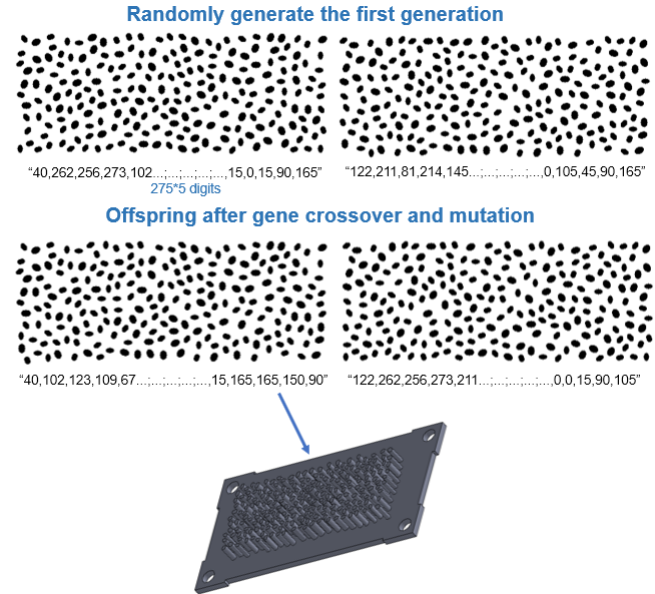


Fig. 4. Illustration of genetic operations for irregular elliptical PinFin

2.2 Evaluation Method

The combination of LBM-LES (Lattice Boltzmann Method - Large Eddy Simulation) with incompressible LBGK can be used to solve the flow velocity field of PinFin. The lattice model employs D2Q9 to calculate convective terms, as illustrated in the Fig. 5. The evolution equation is given by (1), which includes both the collision process and the streaming process.

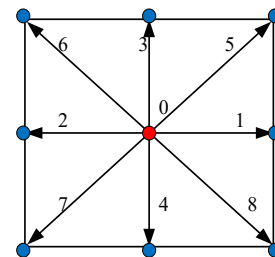


Fig. 5. D2Q9 model in LBM.

$$\underbrace{f_k(x + \Delta x, t + \Delta t) - f_k(x, t)}_{\text{Streaming}} = - \underbrace{\frac{f_k(x, t) - f_k^{eq}(x, t)}{\tau}}_{\text{Collision}} \quad (1)$$

Among them, f is the distribution function at time t at location x , f^{eq} is the equilibrium distribution function, and τ is the relaxation time. According to the eddy viscosity model, τ can be expressed by (2),

$$\tau = 3(v_0 + C\Delta^2|\bar{S}|) + 0.5 \quad (2)$$

Where, v represents the kinematic viscosity and $C\Delta^2|\bar{S}|$ represents the eddy viscosity. C is the Smagorinsky constant, Δ is the Smagorinsky constant, and $|\bar{S}|$ is the modulus of the strain rate tensor \bar{S} .

The velocity and pressure distribution of the water flow can be obtained from (3) and (4).

$$u = \sum_{k=1}^8 c_k f_k \quad (3)$$

$$p = \frac{3c^2}{5} \left[\sum_{k=1}^8 f_k - \frac{2}{3}u \right] \quad (4)$$

where c is Lattice velocity.

When calculating the distribution functions at curved surfaces, the bounce-back method will be utilized, considering all lattice points along the ellipse as the surface. Each directional distribution function can be obtained from the opposite direction distribution function, as shown in (5). As illustrated in the Fig. 6, when dealing with elliptical boundaries, the expression for q is given by (6). Since the D2Q9 model is used, bounce-back boundary treatment needs to be applied to all 8 directions after the stream step.

$$f'_k(x_s, t) = \begin{cases} \frac{1}{2q} f'_k(x_f, t) + \frac{2q-1}{2q} f'_k(x_f, t) & q \geq 0.5 \\ 2q f'_k(x_f, t) + (1-2q) f'_k(x'_f, t) & q < 0.5 \end{cases} \quad (5)$$

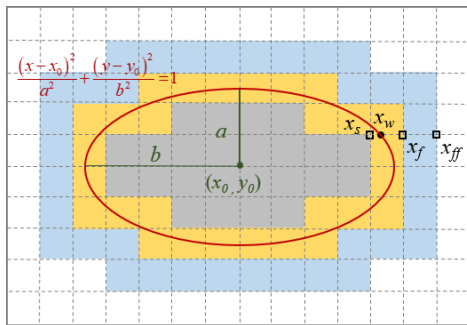


Fig. 6. Elliptical boundary handling method

$$q = \frac{x_f - x_w}{\Delta x} = 1 - \frac{(x_w - x_s)}{\Delta x} = 1 - \frac{a \sqrt{1 - \frac{(y_s - y_0)^2}{b^2}}}{\Delta x} + x_0 \quad (6)$$

The 2.5-dimensional LBM, as illustrated in the Fig. 7, can be used to solve for the junction temperature of the chip. The D3Q7 model is utilized to simulate the heat conduction process, while the D2Q9 combined with D2Q5 models are employed to solve the thermal convection process. This method neglects interlayer convection, thereby accelerating the solution speed. The distribution function is represented by (7), and the equilibrium distribution function is also given by (8).

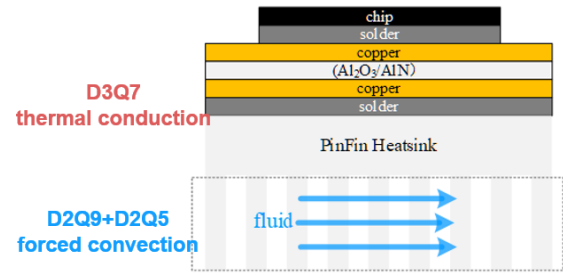


Fig. 7. 2.5D LBM for power module temperature

$$g_k(x + \Delta x, t + \Delta t) - g_k(x, t) = -\frac{1}{\tau} (g_k - g_k^{eq}) \quad (7)$$

$$g_k^{eq} = w_k T \left(1 + \frac{c_k \cdot u}{c_s^2} \right) \quad (8)$$

Where g represents the distribution function of temperature particles in all directions, T is the temperature.

2.3 Optimization Procedure and Result

Different heatsink structures have different operating points. In the optimization process, it is necessary first to determine the flow rate and pressure differential characteristic curve for each candidate structure. This curve is then intersected with the pump characteristic curve to compare the flow speed around the pins at the operating point, which serves as the evaluation criterion. The pump characteristic curve represents the relationship between the flow rate and the head provided by the pump at a specific pump inlet pressure, as shown in Fig. 8. The inlet pressure is proportional to the actual inlet area of the flume. Therefore, the pressure calculated by the LBM needs to be multiplied by a conversion factor before intersecting with the pump curve.

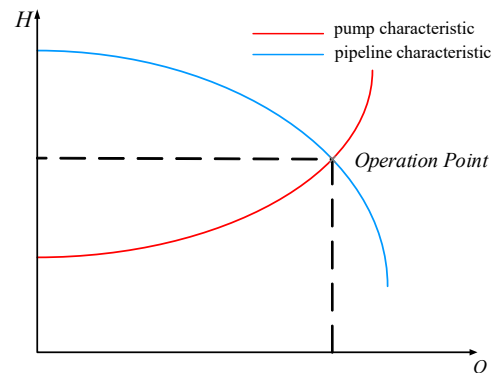


Fig. 8. Pump and pipeline characteristics

Using the proposed optimization method, after a computation time of 51 h, The process of fitness evolution is shown in the Fig. 9.

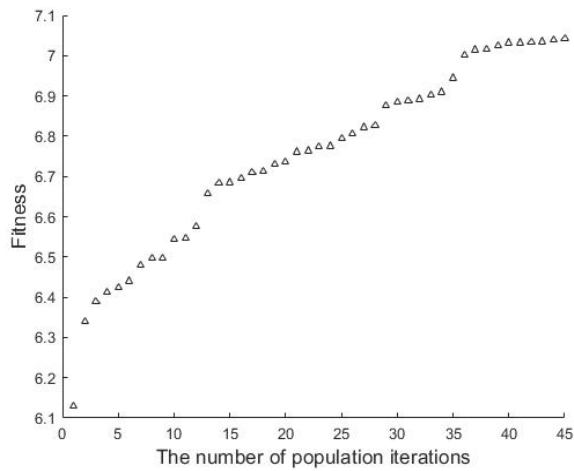


Fig. 9. Genetic algorithm optimization results

The optimized result parameters for the irregular elliptical PinFin heat sink are presented in Table. 1. And Fig. 10 illustrates the velocity distribution and the pressure distribution of the PinFin based on the LBM-LES method.

Table. 1. Optimized result parameters

Parameter	Value
Hate rate (W)	1500
Rate of flow (L/min)	12.64
Pressure (kPa)	28
Junction temperature (°C)	148

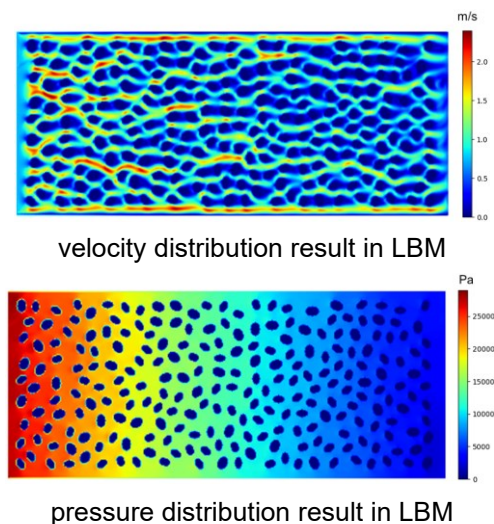


Fig. 10. Optimal result in LBM

To validate the accuracy of the proposed LBM-LESbased evaluation method, the optimal results were verified using Computational Fluid Dynamics (CFD) simulation software. Fig. 11 presents the CFD simulation results, which confirm the accuracy of the proposed evaluation method.

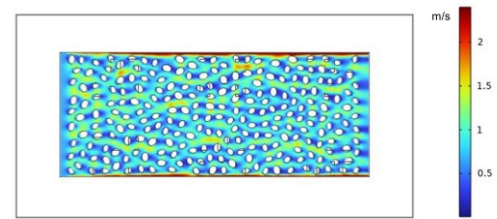
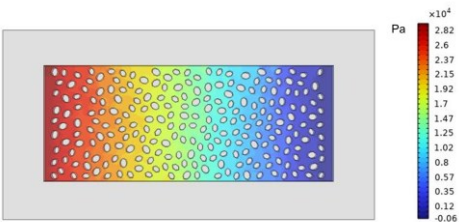


Fig. 11. Result verification in CFD



pressure distribution result in CFD

Fig. 11. Result verification in CFD

A comparison with the optimization results in Ref [11] of regular cylindrical PinFin of the same size, is shown in Fig. 12. It can be observed that the proposed method achieves an improvement of approximately 7°C.

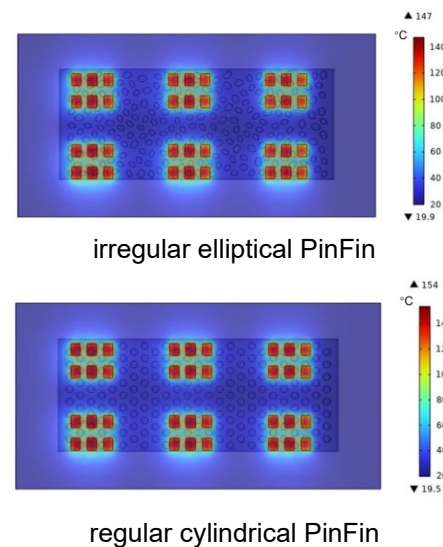


Fig. 12. Optimization result comparison

3 Experimental Verification

Based on the optimized results, an irregular elliptical PinFin heat sink was machined. Subsequently, a high power density three-phase SiC power module based on stacked DBC was fabricated to validate the thermal performance, as illustrated in Fig.13.

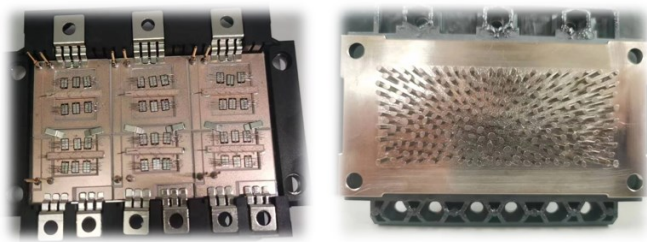


Fig. 13. Manufactured power module with irregular elliptical PinFin.

Simultaneously, the optimal results of the regular cylindrical PinFin heat sink were also machined and welded onto another SiC power module of the same specifications for comparative validation, as shown in Fig. 14.

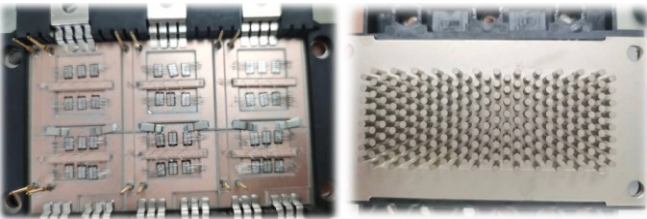


Fig. 14. Manufactured power module with regular cylindrical PinFin.

The experimental environment is illustrated in Fig. 15. Three-phase SiC power modules were connected in series, and a gate voltage was applied to turn on the switch, allowing a large DC current. A water pump drew water from a tank, which flowed through the heat sink to cool the power modules. A flow meter measured the water flow rate. Pressure meter measured the pressure at the inlet and outlet of the heat sink. Note that the readings from the pressure meter do not directly correspond to the simulation pressure results; they are scaled by the ratio of the pipe diameter to the cross-sectional area of the heat sink.

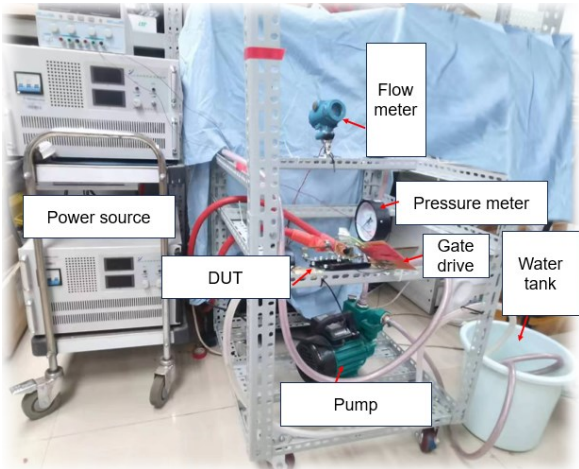
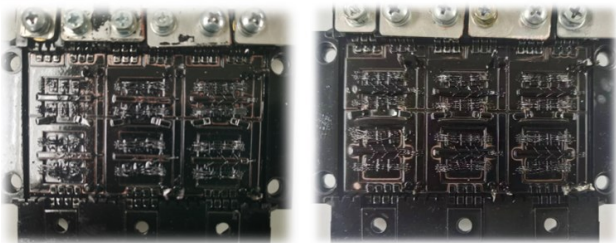


Fig. 15. Experimental environment

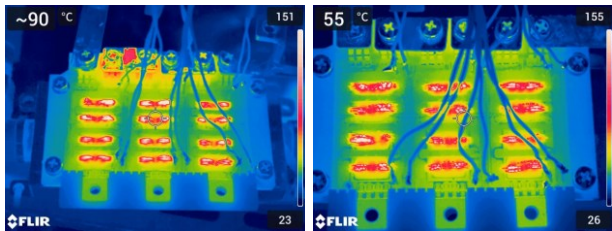
The junction temperature of the three-phase power modules was measured using infrared thermography. To ensure the accuracy of the measurements, no potting process was applied during the fabrication of the power modules, and the surface of the SiC power module was coated with black paint. as shown in Fig. 16.



irregular elliptical PinFin regular cylindrical PinFin

Fig. 16. SiC power module coated with black paint

The temperature distribution experimental results are shown in Fig. 17, and the resulting parameters are presented in Table 2. The pressures listed in the table are converted values. Based on the temperature and loss results, it is evident that the power module equipped with the optimized irregular elliptical PinFin heat sink has a lower junction temperature and lower losses.



irregular elliptical PinFin regular cylindrical PinFin

Fig. 17. Temperature distribution experimental results.

Table. 2. Experimental result parameters

Parameter	Irregular elliptical PinFin	Regular cylinder PinFin
Current(A)	180	180
Rate of flow(L/min)	13.0	14.6
Pressure(kPa)	27	23
Junction temperature(°C)	151	155
Power loss(W)	1368	1432

Due to discrepancies between the manufacturing and design of the heat sinks, there are numerical error between the experimental and simulation results. However, the experimental results still indicate that the optimized irregular elliptical PinFin heat sink results in a

junction temperature that is 4°C lower for the power module, thereby validating the effectiveness of the design method.

4 Conclusion and Discussion

4.1 Conclusion

This paper proposes an automatic optimization method for irregular elliptical PinFin heat sinks based on LBM-LES and genetic algorithms. Compared to existing heat sink optimization methods, this approach offers higher degrees of freedom and is more suitable for high power density SiC power modules. Simulation and experimental validation on stacked DBC three-phase SiC power modules demonstrate that the optimized heat sink outperforms regular cylindrical PinFin heat sinks, achieving lower junction temperatures.

4.2 Discussion

For three-phase SiC power modules, if the same PinFin structure is used for each phase, it will result in the junction temperature of phase A chips near the water inlet being much lower than that of phase C chips near the outlet, as shown in the Fig. 18. This leads to phase A chips not fully exploiting their performance potential, resulting in significant thermal redundancy.

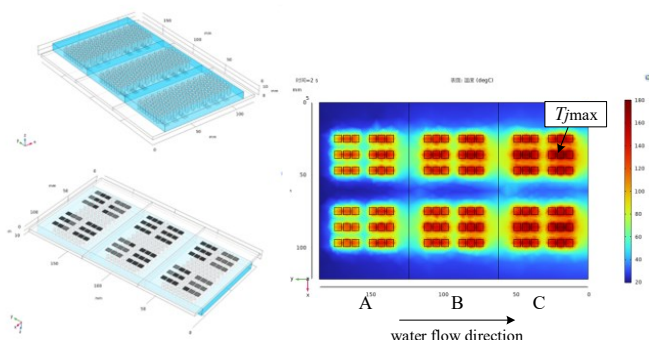


Fig. 18. Temperature distribution result with hot-redundancy

Phase C uses the optimized PinFin layout, and phase B and Phase A reduce 1 and 2 parallel chips, respectively. From the Fig 19, it can be observed that after optimization, the three-phase module can achieve a more evenly temperature. Although the total heat dissipation increases due to the reduction in the number of chips, the maximum chip junction temperature remains unchanged, reducing the cost of thermal redundancy.

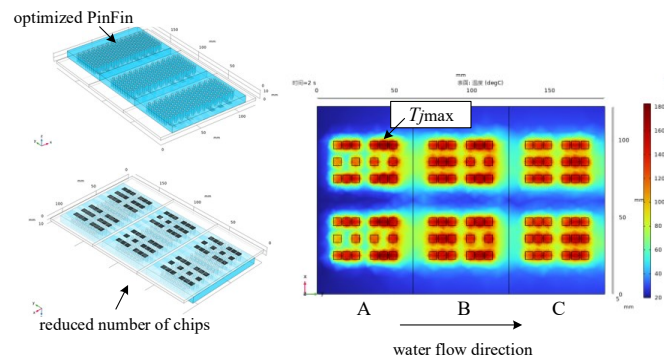


Fig. 19. Temperature distribution results after optimization.

5 References

- [1] Xibo Yuan, Ian Laird, Sam Walder, "Opportunities, challenges, and potential solutions in the application of fast switching SiC power devices and converters," IEEE Transactions on Power Electronics, 2021, pp. 3925-3945.
- [2] Guanhong Song, Bo Cao, Liuchen Chang. Review of Grid-forming Inverters in Support of Power System Operation[J]. Chinese Journal of Electrical Engineering, 2022, 8(1): 1-15.
- [3] Puqi Ning, Xiaoshuang Hui, Yuhui Kang, Tao Fan, Kai Wang, Yunhui Mei, Guangyin Lei. Review of Hybrid Packaging Methods for Power Modules*[J]. Chinese Journal of Electrical Engineering, 2023, 9(4): 23-40.
- [4] J. Azurza, G. Zulauf, J. W. Kolar, G. Deboy, "New figure-of-merit combining semiconductor and multi-level converter properties," IEEE Open Journal of Power Electronics, Vol. 1, pp. 322-338, August 2020.
- [5] D. Ansari, H. Ji, "A novel composite PinFin heat sink for hotspot mitigation," International Journal of Heat and Mass Transfer, 2020, 156, pp. 119-124.
- [6] Pyun S, Cho S, Yoon S W. Analysis of perforated pin design use in automotive SiC power module heatsink[J]. Journal of Power Electronics, 2023, 23(12): 1888-1895.
- [7] Li Kaiyan, Zeng Zheng, Sun Peng. Topology Optimization Design of Pin-Fin for Automotive Power Module [J]. Transaction of China Electrotechnical Society, 38(18): 4963-4977. (in Chinese)
- [8] Gong, Y., Sun, P., Zou, M., Gong, J., & Zeng, Z. (2023, November). Comparative Thermo-Fluid Assessment of Automotive Power Module with Elliptical Pin-Fin. In 2023 IEEE 2nd International Power Electronics and Application Symposium (PEAS) (pp. 1725-1730). IEEE.

- [9] Ramphueiphad S, Bureerat S. Synthesis of multiple cross-section pin fin heat sinks using multiobjective evolutionary algorithms[J]. International Journal of Heat and Mass Transfer, 2018, 118: 462-470.
- [10] Wu T, Wang Z, Ozpineci B, et al. Automated heatsink optimization for air-cooled power semiconductor modules[J]. IEEE Transactions on Power Electronics, 2018, 34(6): 5027-5031.
- [11] Cui J, Ning P, Hui X. Optimization of pinfin heat sink for SiC power module based on LBM-LES[C]//PCIM Asia 2023; International Exhibition and Conference for Power Electronics, Intelligent Motion, Renewable Energy and Energy Management. VDE, 2023: 291-298.